Analysis of lipoprotein transport depletion in *Vibrio cholerae* using CRISPRi

Florence Caro[a], Nicole M. Place[a], and John J. Mekalanos[a,1]

[a]Department of Microbiology and Immunobiology, Harvard Medical School, Boston, MA 02115

Contributed by John J. Mekalanos, June 28, 2019 (sent for review April 10, 2019; reviewed by Joachim Reidl and M. Stephen Trent)

Genes necessary for the survival or reproduction of a cell are an attractive class of antibiotic targets. Studying essential genes by classical genetics, however, is inherently problematic because it is impossible to knock them out. Here, we screened a set of predicted essential genes for growth inhibition using CRISPR-interference (CRISPRi) knockdown in the human pathogen *Vibrio cholerae*. We demonstrate that CRISPRi knockdown of 37 predicted essential genes inhibits *V. cholerae* viability, thus validating the products of these genes as potential drug target candidates. *V. cholerae* was particularly vulnerable to lethal inhibition of the system for lipoprotein transport (Lol), a central hub for directing lipoproteins from the inner to the outer membrane (OM), with many of these lipoproteins coordinating their own essential processes. Lol depletion makes cells prone to plasmolysis and elaborate membrane reorganization, during which the periplasm extrudes into a mega outer membrane vesicle or "MOMV" encased by OM which dynamically emerges specifically at plasmolysis sites. Our work identifies the Lol system as an ideal drug target, whose inhibition could deplete gram-negative bacteria of numerous proteins that reside in the periplasm.

CRISPRi | lipoprotein transport | OMV | *Vibrio cholerae* | plasmolysis

The outer membrane (OM) is an essential structure of gram-negative bacterial cells that functions as a physical barrier to block entry of many classes of antibiotics. The OM also entraps protein components of the periplasmic space, which include enzymes that degrade antibiotics or facilitate their export or efflux from cells. Mutations that disrupt OM integrity reduce virulence in pathogenic bacterial species and increase their susceptibility to antibiotics, suggesting that targeting pathways important for OM maintenance and biogenesis may be a fruitful approach for developing new therapies for bacterial disease (1). Three major complexes are conserved and have central roles in membrane biogenesis of proteobacteria—the lipoprotein transport system (Lol), the Lpt complex, that transports LPS to the surface of the cell, and the Bam complex, that assembles β-barrel OM proteins (2). Both Lpt and Bam complexes rely on the Lol pathway for proper function since it supplies lipoproteins integral to their function. Additionally, OM lipoproteins have roles in peptidoglycan synthesis, virulence (e.g., through their participation in the function of protein secretion systems), and motility. Thus, the Lol system plays a pivotal role in OM integrity and pathogenesis, which makes it an ideal antibacterial drug target.

The Lol system is composed of an ABC transporter, LolCDE, that spans the inner membrane (IM) and, through an energy-consuming step, transfers lipoproteins to LolA. LolA shuttles lipoproteins across the periplasm to the OM-anchored lipoprotein LolB, which inserts them into the inner leaflet of the OM. Lipoproteins contain a characteristic lipobox motif on their N termini, to which the lipid moiety is covalently attached to the conserved cysteine residue (C^{+1}). In *Escherichia coli*, the identity of the +2 residue determines whether lipoproteins are retained or sorted to the OM via the lipoprotein transport system (3, 4). An aspartate at this position causes IM retention whereas most other residues allow trafficking to the OM. The most abundant substrate of the Lol system is also the most abundant protein in *E. coli*—Braun's lipoprotein, or Lpp (5). Anchored in the OM, Lpp is the only known protein that provides a covalent link between the OM and peptidoglycan. LolB depletion causes mislocalization and accumulation of Lpp at the IM, which is lethal to *E. coli* due to aberrant attachment to peptidoglycan (6, 7). It has recently been shown that LolA and LolB are not essential in *E. coli* and only work to prevent the toxic accumulation of lipoproteins, like Lpp, in the inner membrane. This highlights the existence, in *E. coli*, of an alternate lipoprotein trafficking pathway that can transfer substrates from LolCDE to the OM in an LolA and B independent manner (6).

The most commonly deployed antibiotics in bacterial infections target essential gene processes. Essential genes cannot be deleted without genetic complementation or suppression. Robust genetic methods exist that allow the genome-wide assessment of genes for essentiality (8, 9), but the absence of, for example, a transposon insertion in a genomic locus is only an indirect proxy for the essentiality of its encoded product. The recently developed tool CRISPR-interference (CRISPRi) provides an ideal method to transcriptionally silence genes and has been successfully applied to validate and investigate the role of essential genes in bacteria, including *Bacillus subtilis* and *Streptococcus pneumoniae* (10, 11). CRISPRi uses a catalytically inactive form of *Streptococcus pyogenes* Cas9 (dCas9) that lacks endonuclease activity (12). Guided by a single guide RNA (sgRNA), dCas9 is targeted to a genomic locus where it sterically hinders RNA polymerase, thus silencing transcription. The NGG protospacer-adjacent motif (PAM) present on the target locus is necessary for the dCas9–sgRNA complex to bind and inhibit transcription, which can then reduce or "knockdown" expression of encoded gene products.

Here, we applied CRISPRi to knockdown the expression of a set of genes predicted to be essential in *Vibrio cholerae*. Of 37 genes susceptible to knockdown-dependent growth inhibition, *V. cholerae* was found to be most vulnerable to the knockdown of the *lolC* gene encoding lipoprotein transport system component

Significance

In this study, we interrogated the role of *Vibrio cholerae* essential genes in viability and virulence using CRISPR-interference (CRISPRi) and found that depletion of the essential lipoprotein transport pathway causes extrusion of large membrane vesicles and ultimately leads to this pathogen's death. Our work generates mechanistic insights into fundamental areas of *V. cholerae* biology, with important implications for medical prevention of devastating cholera outbreaks.

Author contributions: F.C. and J.J.M. designed research; F.C. and N.M.P. performed research; F.C. contributed new reagents/analytic tools; F.C. and N.M.P. analyzed data; and F.C. wrote the paper.

Reviewers: J.R., University of Graz; and M.S.T., University of Georgia.

The authors declare no conflict of interest.

[1]To whom correspondence may be addressed. Email: john_mekalanos@hms.harvard.edu.

This article contains supporting information online at www.pnas.org/lookup/suppl/doi:10.1073/pnas.1906158116/-/DCSupplemental.

Published online August 1, 2019.

LolC. Live imaging of cells undergoing *lolC* knockdown revealed a series of severe membrane rearrangements that begin with plasmolysis of the IM and end with the extrusion of a large vesicle, filled with periplasm and surrounded by OM, precisely at the site where plasmolysis occurred. These results establish CRISPRi as a powerful tool for examining the effects of gene silencing on *V. cholerae* cell biology and suggest that targeting the Lol pathway for inhibition is likely to have unexpected effects on cells that could enhance drug susceptibility by depletion of periplasmic components.

Results

Development of a CRISPRi System for *V. cholerae*. To develop CRISPRi in *V. cholerae*, we chromosomally integrated the gene encoding dCas9 under the control of an anhydrotetracycline (aTc)-inducible promoter and transformed this strain with a plasmid for constitutive expression of the sgRNA (12) (Fig. 1*A*). Induction of dCas9 with 10 nM aTc was sufficient for inducible and dose-dependent knockdown of two nonessential genes, *tsrA* (*vc0070*) and *luxO*

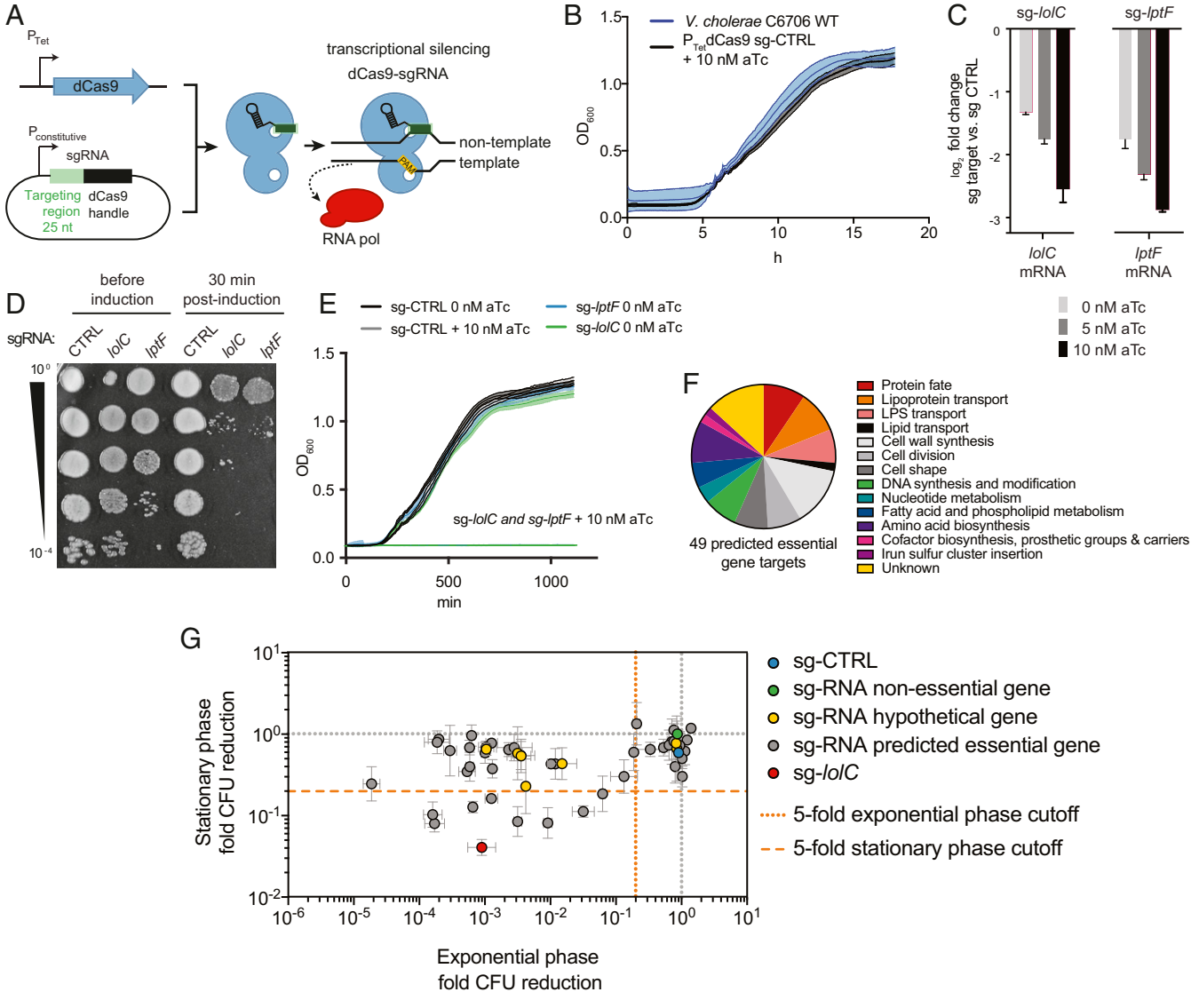

Fig. 1. CRISPRi mediates inducible and dose-dependent knockdown of essential genes in *V. cholerae* with measurable consequences on viability. (*A*) Schematic of the *V. cholerae* CRISPRi system. Catalytically dead dCas9 (blue) in complex with an sgRNA is targeted to the genome and sterically hinders RNA polymerase (red) transcription. The PAM sequence (yellow) is a requirement for the complex to bind, through base complementarity with the sgRNA, to the opposite strand. (*B*) Growth curves of *V. cholerae* wild type (blue) grown in LB medium and sg-CTRL (black) in LB medium with CRISPRi inducer (10 nM aTc). Data represent the average of 4 biological replicates. (*C*) *LolC* and *lptF* gene knockdowns quantified by qRT–PCR at 30 min post-CRISPRi induction with increasing amounts of inducer. Error bars are SDs of three technical replicates. (*D*) The consequences of CRISPRi gene knockdown were monitored by spotting 10-fold serial dilutions of each culture before and after 30-min induction with 10 nM aTc. (*E*) *V. cholerae* sg-CTRL (black), sg-*lolC* (green), and sg-*lptF* (blue) grown in the presence or absence of 10 nM aTc. Data represent the average of 4 biological replicates. (*F*) The set of predicted essential genes listed in Dataset S1 were selected to span a range of functional categories. (*G*) *V. cholerae* viability upon CRISPRi induction of each of the predicted known and hypothetical essential genes (gray and yellow, respectively), a nonessential gene (green), or an empty guide RNA sg-CTRL was assessed in exponential (*x* axis) and stationary phase (*y* axis). For the exponential phase dataset, CFUs were counted by 10-fold serial dilution spotting on plates with and without CRISPRi inducer. CFUs of stationary phase bacteria were counted by 10-fold serial dilution spotting after incubating cells with and without inducer for 5 h. Gray dotted lines intersect at 1-fold; i.e., no change in CFUS. To the left and below of the orange dotted and dashed lines, respectively, are targets for which the fold CFU reduction in exponential and stationary phase, respectively, is higher than 5-fold, including *lolC* (red). The fold CFU reduction is the ratio of induced to uninduced CFU counted. Error bars are SEM of three biological replicates.

(*vc1021*). As expected, knockdown of *tsrA* or *luxO*, either individually or simultaneously, induced transcription of operons involved in Type VI Secretion System (T6SS) function, as has been previously reported for null mutations in these loci (13) (*SI Appendix*, Fig. S1*A*). Consistent with published work (12), the highest knockdown efficiencies were obtained with sgRNAs targeting the nontemplate strand closest to the 5′ end of coding regions, with a maximum 18.5-fold reduction in *tsrA* transcript levels (*SI Appendix*, Fig. S1*B*). To increase specificity and reduce the number of off-target effects, most sgRNAs were designed with a 25-nt targeting sequence; however, shorter 20-nt sequences also mediate efficient knockdown, as observed for sg-*vc2395*, sg-*vca0921*, and sg-*vc1246*. No growth defects were detected for the CRISPRi strain in the presence of inducer and a control sgRNA without a targeting sequence (sg-CTRL), or an sgRNA targeting a nonessential gene, compared with the wild-type parental strain (Fig. 1*B*). In contrast, CRISPRi knockdown of two predicted essential genes, *lolC* (*vc1884*), encoding the OM-specific lipoprotein transporter subunit C, and *lptF* (*vc2500*), encoding lipopolysaccharide export system permease protein LptF, completely inhibited bacterial growth (Fig. 1*D*). A reduction of 5.8- and 7.3-fold for *lolC* and *lptF* transcript levels, respectively, caused an ∼1,000-fold reduction in colony-forming units (CFUs) within 30 min of CRISPRi induction, indicating that, for these genes, even a relatively low (<10-fold) reduction in mRNA abundance is sufficient to cause significant growth inhibition and/or cell death (Fig. 1 *C*–*E*). We observed a 2- to 3-fold knockdown in the absence of inducer in the sg-*lolC* and sg-*lptF* strains (Fig. 1*C*). While this leakiness was well tolerated by sg-*lolC*, it caused an ∼10-fold reduction in CFUs in the sg-*lptF* strain (Fig. 1 *D* and *E*). The growth curves obtained for sg-*lolC* and sg-*lptF* in the absence of inducer were indistinguishable from sg-CTRL. These results establish CRISPRi as a powerful tool for examining the effects of gene expression knockdown in *V. cholerae*.

Use of CRISPRi to Probe the Essentiality of Selected *V. cholerae* Genes. We next applied the CRISPRi system to silence 53 genes predicted to be essential in the Chao et al. (9) Transposon insertion sequencing (Tn-seq) analysis, expressed in Luria–Bertani (LB), conserved (unless hypothetical), and representing a range of biological functions, including cell wall synthesis, cell division, protein and lipid transport, protein fate, metabolism, and DNA synthesis and modification, as well as seven genes annotated as hypothetical with unknown function (Fig. 1*F* and Dataset S1). First, we monitored the effects of gene knockdown on *V. cholerae* viability. For this, we grew each of the strains to exponential phase and determined CFUs by serial dilution plating on medium with (+aTc) or without the dCas9 inducer. While viable counts of the strains carrying either the sg-CTRL or an sgRNA targeting the nonessential gene *tsrA* were unaffected, those of 33 strains with sgRNAs targeting predicted essential genes were reduced by at least 5-fold in the presence of inducer, indicating that *V. cholerae* is vulnerable to depletion of the corresponding gene products (Fig. 1*G*). Mutations arising either in the CRISPRi machinery per se (14) together with bona fide extragenic supressors of the target genes can give rise to "escape" mutants that grow in the presence of CIRSPRi inducer (15). Indeed, we confirmed the presence of frameshift mutations in the dCas9 gene for the sg-*lptB*, sg-*lptF*, and sg-*vc0842* strains displaying no growth defect (*SI Appendix*, Fig. S2). Knockdown of the putative IM protein translocase component *yidC* (*vc0004*) and the lipopolysaccharide export system protein A *lptA* (*vc2527*) displayed the largest reduction in CFUs (∼53,000- and ∼6,000-fold, respectively). Knockdown of 5 of the 7 hypothetical genes with unknown function also significantly affected viability. Protein structure homology analyses predict 4 of these proteins to be involved in metabolic and nucleic acid catabolism processes and 1 in protein quality control (Dataset S2). The knockdown of none of these genes resulted in a discernible morphological phenotype (Movies S1–S4).

We next monitored growth for 12 replicate cultures (3 biological replicates containing 4 technical replicates per query gene) of each of the 33 strains displaying the largest reduction in CFUs on plates containing the dCas9 inducer. While all strains displayed a growth defect in the presence of aTc, escape mutants were frequently observed (*SI Appendix*, Fig. S3). Despite this propensity, we observed no escape mutants for strains expressing sgRNAs targeting *ftsY*, *lolC*, and *vc2395*. In summary, of the 53 predicted essential genes reported by Chao et al. by Tn-Seq, we were able to confirm 37 by CRISPRi, of which 31 were also predicted to be essential by Kamp et al. by Tn-Seq (16) (*SI Appendix*, Fig. S4 and Dataset S1).

In nutrient-limiting conditions, bacteria enter stationary phase, during which they scarcely divide, exhibit low metabolic activity, and become notoriously hard to kill with antibiotics (17). To evaluate how knockdown of our set of predicted essential genes would impact *V. cholerae* viability under these conditions, we split stationary phase cultures grown overnight in two and either mock treated or exposed the culture to 50 nM aTc inducer, for 5 h. We determined the fold decrease in viable bacteria after aTc treatment by counting CFUs through serial dilution plating. We found that, for every gene targeted, the magnitude of CFU reduction was smaller than the one measured in exponential phase bacteria, likely due to CRISPRi-mediated knockdown being less efficient during this growth phase. Nevertheless, the knockdown of 9 genes caused at least a 5-fold decrease in CFUs (Fig. 1*G*). Six of these genes (*mreC*, *rodA*, *murG*, *mrdA*, *lptA*, and *lptF*) are involved in cell envelope biogenesis, and the remaining three (*pbp3*, *secY*, and *lolC*) are involved in cell division, protein export, and lipoprotein transport, respectively. Knockdown of *lolC* in stationary phase was the most detrimental to *V. cholerae* viability, causing a 25-fold reduction in CFUs. No significant correlation was found between the data collected in stationary versus exponential phase, indicating that gene product levels required to support growth are different in each of these phases. Neither did we find a correlation between the expression levels of a gene and the impact on viability upon knockdown, indicating that knockdown efficiency is independent of promoter strength (*SI Appendix*, Fig. S5). These results demonstrate that CRISPRi knockdown can be used to identify promising drug targets in *V. cholerae* that are particularly vulnerable to inhibition, including when cells are in stationary phase and thus resistant to killing by many antibiotics, such as β-lactams and quinolones (17). Additionally, we show that *V. cholerae* is especially sensitive to depletion of lipoprotein transport both during exponential and stationary phase.

mRNA Depletion of Any of the Lol System Components Causes Loss of *V. cholerae* Viability. Taking advantage of our CRISPRi system, we sought to further characterize the role of Lol system depletion on *V. cholerae* toxicity. We first designed sgRNAs targeting each of the Lol components and found that *V. cholerae* growth was severely inhibited when plating these strains on medium containing the CRISPRi inducer (Fig. 2*A*). Additionally, the growth defect caused by *lolC* knockdown was completely rescued in a PAM_{mut} strain in which the cognate PAM sequence for sg-*lolC* is mutated, indicating that the defect measured is specific to the *lolC* knockdown and not an sgRNA off-target nor a CRISPRi-independent effect. To better understand the dynamics of cell death during Lol system knockdown over time, we measured the reduction in CFUs post-CRISPRi induction for each of its components. Within 10 min of CRISPRi induction, viable counts were reduced by 70-fold in the *lolC* knockdown. A much smaller effect was observed for *lolA*, *lolB*, *lolD*, and *lolE*, where the CFU reduction was between 1- and 5-fold 10 min postinduction. At 60 min postinduction, viable counts for *lolC*,

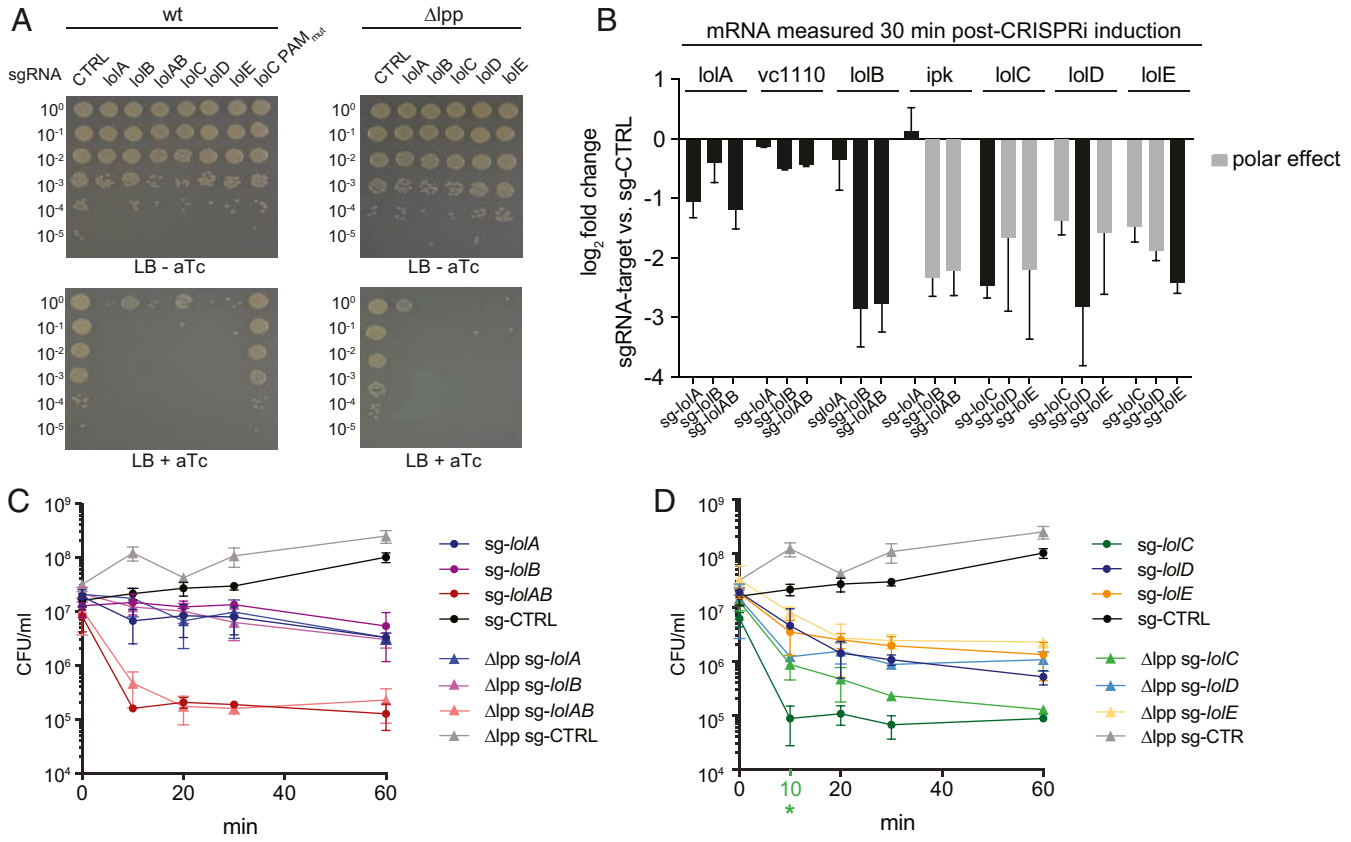

Fig. 2. Knockdown of any of the Lol system components is detrimental to *V. cholerae* viability, and the absence of its major substrate Lpp does not alleviate this effect. (*A*) *V. cholerae* wild type or Δlpp expressing sgRNAs targeting each of the Lol system components or multiplexed to target both *lolA* and *lolB* simultaneously were serially diluted by 10-fold and spotted on medium with (+aTc) or without (−aTc) CRISPRi inducer. (*B*) Knockdown level exerted on each of the genes in the corresponding operons by each of the indicated sgRNAs was quantified by qRT–PCR at 30 min post-CRISPRi induction. Polar effects are highlighted in gray. Error bars are SDs of three technical replicates. (*C* and *D*) *V. cholerae* wild type or Δlpp viability after Lol system knockdown over time. The green asterisk indicates a significant difference between the wild type and the mutant sg-*lolC* strain at 10 min (*t* test, $P < 0.05$). Error bars are SDs of three biological replicates.

lolD, and *lolE* knockdown strains were 71-, 36-, and 14-fold lower than the controls, but this longer period of knockdown for *lolA* and *lolB* individually did not further enhance loss of viability, compared with the shorter induction period. In contrast, simultaneous knockdown of *lolA* and *lolB* resulted in 50- and 64-fold reduction in viable CFUs within 10 and 60 min, respectively (Fig. 2*C*). CRISPRi knockdown has been reported to be polar, and thus any gene downstream of the dCas9–sgRNA complex binding site in an operon might be silenced (12). As expected, we detected polar effects on *lolD and lolE* transcript levels by sg-*lolC* and sg-*lolD*, respectively as these genes are encoded in the *lolCDE* operon. While sg-*lolB* exerts a polar effect on the predicted essential gene immediately downstream (*ipk*, *vc2182*), no polar effect was observed on the predicted essential gene *vc1110* encoded last and downstream of *lolA* (Fig. 2*B* and *SI Appendix*, Fig. S6). As reported for *E. coli* and *B. subtilis* (10, 18), we also observed CRISPRi upstream polarity in the *lolCDE* operon where targeting *lolD* and *lolE* also causes knockdown of the upstream genes *lolC* or *lolC* and *lolD*, respectively (Fig. 2*C*). These data show that even low levels of depletion (2- to 7-fold at 30 min postinduction) of any of the Lol system components are detrimental to *V. cholerae* viability and that this effect is likely exacerbated through polarity on operons that carry multiple essential genes and/or through the need for these gene products to functionally interact.

We next asked whether the lethality observed upon Lol system knockdown could be due to toxic accumulation of lipoproteins at the IM or to increased membrane permeability. In *E. coli*, when LolB is depleted, the major substrate of the Lol system, Lpp, accumulates in the IM, and this was demonstrated to be toxic (6). To explore this possibility in *V. cholerae*, we tested viability in a Δlpp mutant upon knockdown of each of the Lol system components. The absence of Lpp did not rescue the terminal phenotype observed in any of the Lol system knockdown strains. A small but statistically significant ($P < 0.05$) difference was observed during the first 10 min of *lolC* knockdown where it caused ~70-fold reduction in CFUs in the wild type, compared with only 15-fold in the Δlpp mutant (Fig. 2*C*). At 60 min post-*lolC* knockdown, the CFUs recovered in wild type, and Δlpp converged to equal numbers. Thus, while Lpp accumulation in the IM during early stages of *lolC* knockdown may lead to toxicity, it is unlikely to be the major determinant of cell death during Lol system depletion.

The OM of gram-negative bacteria shows low permeability to large or hydrophobic antibiotics, primarily as a result of its highly hydrophobic lipid bilayer and its OM porins with restrictive channel diameters (1). Loss of OM stability can therefore have a major impact on the susceptibility to antibiotics which target intracellular processes. To examine OM perturbation, we tested *V. cholerae* susceptibility to the hydrophobic antibiotic novobiocin and the large antibiotics vancomycin and bacitracin, as well as bile salts and the detergent SDS, in the context of lipoprotein, LPS transport, and Bam complex knockdown. For this, we designed two additional sgRNAs against *lptE* and *bamA* (sg-*lptE_2* and sg-*bamA_2*) with a

stronger effect on *V. cholerae* viability (−4.7 and −3.0 $\log_{10}$ fold CFU reduction, respectively) than the ones used in our original screen (−0.87, and −0.68 $\log_{10}$ fold CFU reduction, respectively). Because full knockdown of these targets is lethal, the effect of each compound is obscured when using 10 nM aTc. We therefore evaluated the *V. cholerae* susceptibility of each compound at basal level knockdown in the absence of aTc. In the absence of treatment, all strains grew as much as the sg-CTRL; however, basal knockdown of *lolC*, *lptE*, and *bamA* sensitized cells to 0.2% bile, 0.05% SDS, 50 μg/mL vancomycin, and 3.75 μg/mL novobiocin, but not the range of bacitracin concentrations tested (50 to 400 μg/mL) (*SI Appendix*, Fig. S7). These results indicate that, when lipoprotein, LPS transport, or β-barrel protein assembly are impaired, the OM is perturbed such that large or hydrophobic antibiotics, like

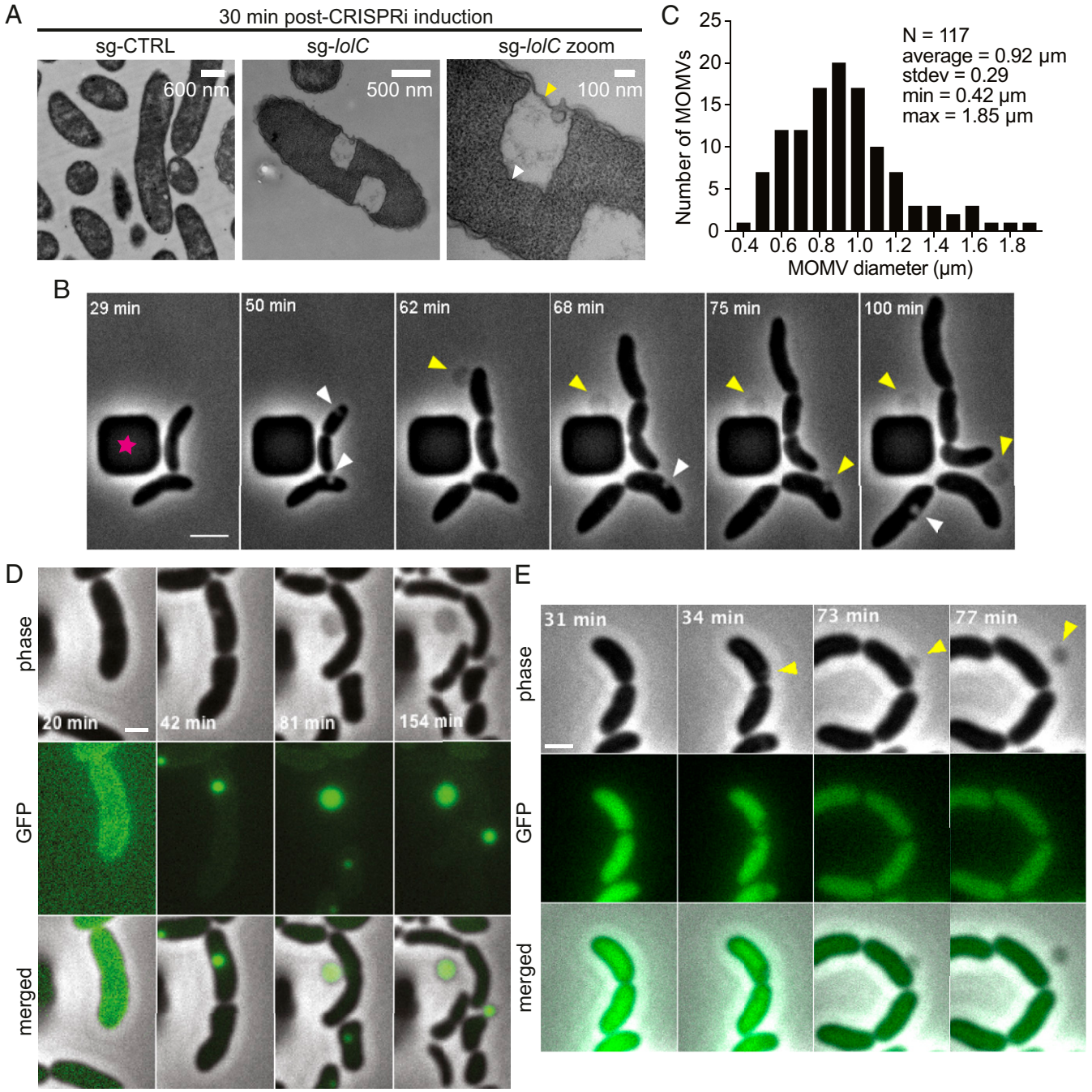

Fig. 3. *lolC* knockdown predisposes *V. cholerae* to undergo plasmolysis and causes the OM to extrude into a periplasm-filled MOMV. (*A*) Electron micrographs of *V. cholerae* sg-CTRL and sg-*lolC* fixed 30 min after CRISPRi induction. White and yellow arrowheads in the zoomed image point to the retracted IM forming an enlarged plasmolysis bay and the OM, respectively. (*B*) *V. cholerae* sg-*lolC* bacteria trapped in the microfluidics chamber exposed to medium with CRISPRi inducer and imaged over time (Movie S7). The phase dark squares (magenta star) are part of the microfluidics device. White arrowheads point to plasmolysis bays formed early during treatment. Yellow arrowheads point to MOMVs extruding from cells at the precise location where plasmolysis bays formed and remaining stable over time. (*C*) MOMV size distribution ($n = 117$). (*D*) *V. cholerae* sg-*lolC* expressing periplasmic sfGFP imaged over time extruding a periplasm-filled green fluorescent MOMV (Movie S10). (*E*) *V. cholerae* sg-*lolC* expressing cytoplasmic sfGFP imaged over time (Movie S13). Yellow arrowheads point to the phase dark MOMV extruding from cells at plasmolysis sites. (Scale bars: *B*, 4 μm; *D*, 1 μm; *E*, 1 μm.)

vancomycin and novobiocin, become permeable and cells are more susceptible to the detergent properties of amphipathic bile salts and SDS. Additionally, knockdown of any of the Lol system components rendered cells more susceptible to 0.5 mM NaCl than either the sg-CTRL or PAM_{mut} strains (*SI Appendix*, Fig. S8). These results indicate that compromised OM permeability contributes at least in part to *V. cholerae* lethality upon *lolC*, *lptE*, and *bamA* knockdown.

Knockdown of *lolC* Causes Dynamic Membrane Perturbations. CRISPRi offers an ideal tool to examine whether knockdown of essential gene expression affects cell structures in observable ways. To inspect the phenotypic consequences of *lolC* knockdown on cell morphology, we used electron microscopy. The morphology of the sg-CTRL strain, in the presence or absence of CRISPRi inducer, was indistinguishable from that of wild-type *V. cholerae* (*SI Appendix*, Fig. S9*A*). In contrast, the *lolC* knockdown displayed severe morphological defects including lysis, filamentation, and IM invaginations that formed large periplasmic pockets (Fig. 3*A*). In many cases, more than one periplasmic pocket was visible per cell, particularly in filamentous cells (*SI Appendix*, Fig. S9*B*). This membrane morphology is reminiscent of plasmolysis, a process typically caused by cells adjusting to hyperosmotic shock. Plasmolysis has been shown to occur in *V. cholerae* and can be induced by culturing cells in the presence of high solute concentrations (19). Under these conditions, water is lost from the cytoplasm, and the IM retracts from the cell envelope (i.e., the peptidoglycan and OM), generating periplasmic pockets that bulge into the cytoplasm, forming plasmolysis bays. We reasoned that, if *lolC* knockdown sensitizes cells to undergo plasmolysis, we would be able to observe this phenotype by exposing live bacteria to hyperosmotic shock or to a membrane-destabilizing agent. To test this, we first engineered our strains to express superfolder GFP (sfGFP) in the periplasm (^{SS}dsbA-sfGFP), which allows for better visualization of plasmolysis bays using fluorescence microscopy (20). Next, we imaged *V. cholerae* sg-CTRL and sg-*lolC* on agarose pads containing either 0.5 M NaCl, 400 mM sorbitol, 15% sucrose, or 0.1 mM EDTA. While none of the treatments caused sg-CTRL to plasmolyze, we observed a range of about 7 to 50% of plasmolyzed cells for the sg-*lolC* strain. Exposure to 15% sucrose or 0.5 M NaCl yielded the highest number of plasmolyzed cells (42% and 50%, respectively), followed by 400 mM Sorbitol and 1× PBS (21% and 29%, respectively), and 0.1 mM EDTA and no treatment (7%) (*SI Appendix*, Figs. S10 and S11). Remarkably, plasmolysis occurs in the absence of high solute concentration and in the presence of 1× PBS, indicating that even low levels of *lolC* knockdown can cause the IM to retract from the cell envelope and that, while changes in osmolarity or membrane-destabilizing agents can exacerbate this response, they are not required to observe this phenotype. Finally, some of the cells without visible plasmolysis bays displayed a bulge that extended away from the cell body (*SI Appendix*, Fig. S11*C*). These bulges displayed bright green fluorescence, indicating that their contents likely included periplasmic components such as ^{SS}dsbA-sfGFP.

To further explore the underlying mechanism of plasmolysis, we tested whether independent knockdown of the LPS transport system and the BAM complex, both relying on essential lipoproteins transported by the Lol system, would result in plasmolysis bay formation. No plasmolysis was observed in the sg-*lptE_2* and sg-*bamA_2* knockdowns, compared with 6.4% of cells displaying plasmolysis bays upon *lolC* knockdown (*SI Appendix*, Fig. S12). Thus, impaired LPS transport or β-barrel protein assembly on the OM alone does not sensitize cells to undergo plasmolysis, indicating that, in order for plasmolysis to occur, either both systems need to fail simultaneously or retention in the IM of any of the other *V. cholerae* lipoproteins is required. Globomycin is a cyclic peptide antibiotic, which inhibits the lipoprotein signal peptidase LspA that converts prolipoprotein to lipoprotein, which in turn causes the toxic accumulation of prolipoprotein in the IM (21). *V. cholerae* is not only susceptible to globomycin, but globomycin-treated sg-CTRL cells fully recapitulated the *lolC* knockdown phenotype as both plasmolysis bays and bulges were observed (*SI Appendix*, Fig. S13 and Movies S5 and S6). These data confirm that lipoprotein accumulation in the IM is necessary for the observed phenotype.

Plasmolysis bays and the observed bulges could arise either as a consequence of the same or distinct/independent physical processes acting in different cells. To discriminate between these two possibilities, we monitored dynamic changes in cell shape during *lolC* knockdown using time-lapse microscopy on cells physically immobilized in a microfluidics chamber. Trapped cells were exposed to a continuous supply of medium and monitored during controlled shifts from rich to modified medium. This allowed us to control the timing and duration of the shift in chemical composition of the media experienced by *lolC*-depleted cells while simultaneously recording the effects on cell growth and morphology. We found that, in *lolC*-depleted cells, plasmolysis bays form and remain intact during the 2-min shift to 1× PBS but ultimately do resolve (Movie S7 and Fig. 3*B*). Notably, continued monitoring of these cells after the osmotic shock revealed a large spherical vesicle or mega outer membrane vesicle (MOMV) extruding from the cells precisely at the location at which plasmolysis bays had formed. These MOMVs were on average 0.9 μm in diameter, with the largest one detected being 1.85 μm (Fig. 3*C*). No morphological changes were observed in the sg-CTRL strain nor in the sg-*lolC* strain that carried a mutated PAM on the *lolC* genomic locus (Movies S8 and S9). These data suggest that Lol system knockdown not only makes cells prone to plasmolysis but also causes dynamic membrane rearrangements that resolve morphologically with the formation of an MOMV precisely at the sites where the inner and OM retract during plasmolysis.

To better understand MOMV formation, we evaluated their origin, contents, and membrane composition. For this, bacteria expressing either periplasmic or cytoplasmic sfGFP were continuously exposed to CRISPRi inducer and shifted for 2 min to a medium with 0.1 mM EDTA to induce plasmolysis. Bright fluorescent plasmolysis bays filled with periplasmic sfGFP appeared immediately when monitoring the *lolC* knockdown following EDTA treatment, and the MOMVs extruded at these sites were green fluorescent, indicating that these are filled with periplasm (Fig. 3*D* and Movie S10).

Fluorescent green plasmolysis bays and MOMVs were also detected for the *lolA* and *lolB* knockdowns when subjected to the same treatment (Movies S11 and S12), but this was not the case for the sg-*lolC* strain with a mutated PAM in the *lolC* genomic locus (Movie S9) nor for cells expressing cytoplasmic sfGFP, which, upon *lolC* knockdown, showed phase bright bays and nonfluorescent MOMVs (Fig. 3*E* and Movie S13). Strikingly, in every case, the MOMV extruded at the precise site at which a plasmolysis bay had formed, linking these two physical processes in time and space; plasmolysis bay formation precedes MOMV formation and MOMVs form at plasmolysis sites. To examine the origin of the membrane that surrounds the MOMV, we used the N terminus of *V. cholerae* Lpp fused to mCherry (^{SS}lpp-mCherry) to fluorescently label the OM (Fig. 4*A*). The mCherry fusion protein expressed in *E. coli* and *V. cholerae* bacteria delineated the cell circumference brightly and was more diffuse in the center, indicating that the construct localizes to the periphery of the cell (*SI Appendix*, Fig. S14). At the beginning of the experiment, mCherry was uniformly localized to the periphery in both sg-CTRL and the sg-*lolC* strains expressing cytoplasmic sfGFP (Fig. 4 *B* and *C*). After EDTA treatment, however, the sg-*lolC* knockdown displayed phase bright plasmolysis bays from which a fluorescent red MOMV was extruded, indicating that the membrane

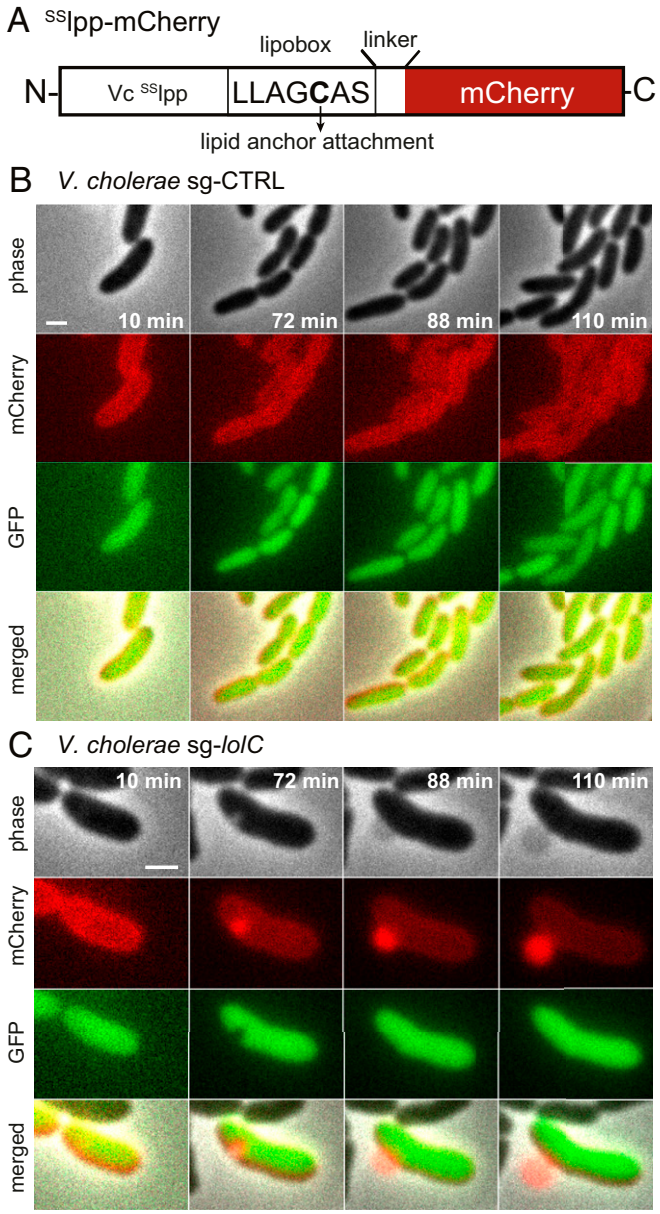

Fig. 4. The MOMV is surrounded by OM. (*A*) Schematic of the ^{SS}lpp-mCherry construct. The N terminus of *V. cholerae* Lpp (Vc ^{SS}lpp), including the lipobox motif, is followed by a linker and the red fluorescent protein mCherry. Shown are time-lapse microscopy images of *V. cholerae* (*B*) sg-CTRL (Movie S15) and (*C*) sg-*lolC* expressing sfGFP in the cytoplasm and OM-anchored mCherry (Movie S14). (Scale bars: 1 μm.)

surrounding it contains OM (Movie S14 and Fig. 4*C*). No plasmolysis nor MOMVs were observed in the sg-CTRL strain (Movie S15 and Fig. 4*B*). Because the ^{SS}lpp-mCherry itself relies on the Lol system for transport to the OM, a fraction will remain trapped at the IM upon knockdown (which may also exacerbate toxicity), and thus we cannot fully discard the possibility that some of the fluorescent label surrounding the MOMV was derived from the IM. To further examine the presence of OM surrounding MOMVs, we used a fluorescent polymyxin derivative, Dansyl-polymyxin B nonapeptide (D-PMBN), previously shown to specifically bind LPS in gram-negative bacterial membranes (22). D-PMBN fluorescence localized to the MOMV surface as visualized using fluorescence microscopy (*SI Appendix*, Fig. S15), highlighting the presence of OM LPS on the MOMV surface.

Bacteria produce and release outer membrane vesicles (OMVs), which are derived from the cell envelope and carry soluble periplasmic contents (23), and *V. cholerae* OMVs appear to be similarly loaded with periplasmic proteins such as DegP (24). OMVs are thought to provide a means for the cell to relieve stress by disposing of toxic molecules, highly overexpressed, or misfolded proteins, that accumulate in the periplasm under stress conditions. Beyond reducing the toxic burden in the periplasm, OMVs have been shown to package active periplasmic enzymes that mediate antibiotic protection like β-lactamases (25). To explore the intriguing possibility that the observed MOMV would package periplasmic contents that accumulate when Lol system function is impaired, we took advantage of the β-lactamase expressed from the sgRNA plasmid. This enzyme localizes to the periplasm and confers resistance to the β-lactam carbenicillin. If the MOMV packages and depletes this enzyme from the periplasm, then Lol system knockdown would render these bacteria more sensitive to carbenicillin. Indeed, at basal levels of *lolC* knockdown, *V. cholerae* was more sensitive to carbenicillin than the sg-CTRL, and *lolC* knockdown rendered bacteria up to 24-fold more sensitive to carbenicillin when quantitated in liquid killing assays (Fig. 5). Because hypersensitivity to β-lactams could also be due to OM disruption in the *lolC* knockdown, we tested carbenicillin sensitivity of the *lptE* and *bamA* knockdowns, shown to not produce MOMVs. While the effect of carbenicillin treatment on the *lolC* knockdown was larger (3.4- and 8.8-fold reduction in CFUs in the presence of carbenicillin without and with aTc, respectively), the *bamA* knockdown also showed a slight defect in viability (2.6- and 1.7-fold reduction in CFUs in the presence of carbenicillin without and with aTc, respectively) (*SI Appendix*, Fig. S16), indicating that disruption of the OM in the *lolC* knockdown could also contribute to increased carbenicillin sensitivity in this strain.

Discussion

Here, we report the use of CRISPRi in *V. cholerae* and its application to probe the essentiality of 53 *V. cholerae* genes. Using a single sgRNA, we achieved inducible and dose-dependent transcriptional knockdown of either essential or nonessential genes. In bacteria, mRNA levels are generally correlated with protein levels (26). The striking lethality achieved with even mild knockdown for most of the targeted genes suggests that, in *V. cholerae*, their encoded proteins exist at levels that are just enough to support growth and that the threshold of mRNA molecules required to sustain life is narrow, at least in the case of *lolC* and *lptF*, where 2- to 3-fold knockdown is not sufficient to significantly affect growth but 8-fold is. In contrast, reducing the

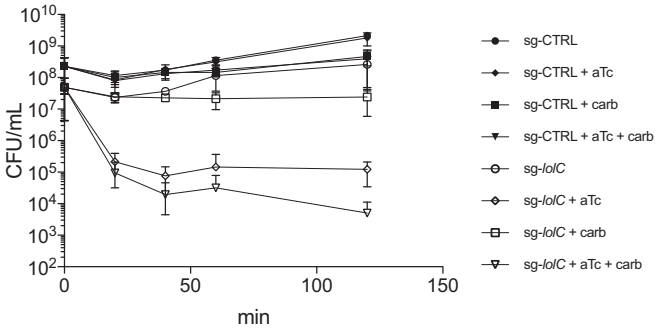

Fig. 5. Knockdown of lolC increases *V. cholerae* sensitivity to β-lactams. *V. cholerae* sg-CTRL or sg-*lolC* CFUs were monitored over time either in the absence (circles) or the presence of 500 μg/mL β-lactam carbenicillin (carb, squares), or the presence of CRISPRi inducer (aTc, diamonds), or the presence of both (triangles). Error bars indicate SDs of 3 biological replicates performed on separate days.

expression levels of some essential genes by more than 97% has little or no effect on the growth or viability of *Mycobacterium* species (27, 28). Thus, the predicted essential genes studied here represent a highly vulnerable set of targets for *V. cholerae* and perhaps other gram-negative bacteria. Although no growth defect was observed for 16 of the targeted genes, it seems probable that this simply reflects the failure of the CRISPRi system to repress these genes sufficiently to cause cell death or the existence of suppressor mutations. The observed leakiness of the system may contribute to the accumulation of suppressor mutations before functional assays are performed and could explain, in part, why suppressors arise so quickly when cultures are inoculated heavily with cells grown without inducer. Failure to knock down could also be due to weak dCas9 repression since it has been shown that the dCas9 complex can be displaced by RNA polymerase or during DNA replication, particularly when sgRNA base pairing is weak (29). Given the small sequence requirement of the PAM, it is possible to design higher affinity sgRNAs and/or simultaneously target genes with multiple sgRNAs to test their essentiality. Indeed, we achieved higher levels of *lptE* and *bamA* knockdown lethality when using two redesigned sgRNAs against these genes (sg-*lptE*_2 and sg-*bamA*_2). While the precise sgRNA design rules for efficient gene knockdown in *V. cholerae* remain to be determined, here, we show a 70% success rate using one sgRNA per target. Despite these challenges, CRISPRi provides several advantages over conventional genetic manipulation in bacteria that include the following: the depletion of essential gene products while under the regulation of their native promoters and without perturbing the genome, fewer resources and time spent on construction of multiple deletion strains, and easy multiplexing of different sgRNAs for simultaneous knockdown of different genes to generate complex phenotypes (15).

Of the genes targeted in this study, *V. cholerae* was most susceptible to knockdown of *lolC*, and this susceptibility extended to all Lol system components. In *E. coli*, highly efficient lipoprotein transport via LolB is demanded by the production of Lpp and OsmB since mislocalization to the IM of these two lipoproteins leads to toxicity (6). In *V. cholerae lolC* knockdown, toxicity is not alleviated in the absence of Lpp, suggesting that *V. cholerae* can tolerate Lpp accumulation at the IM and that other mechanisms are at play that culminate in cell death. OsmB is expressed in *E. coli* as a consequence of inappropriate localization of the lipoprotein RcsF to the IM, which in turn activates the cell envelope stress response, Rcs (6). While neither OsmB nor the Rcs pathway are conserved in *V. cholerae*, it is possible that aberrant accumulation at the IM of one of the other 53 lipoproteins encoded in the *V. cholerae* genome (30) is responsible for the observed toxicity of Lol system knockdown.

Because of its central role in supplying the OM with lipoproteins, many of which are themselves essential, interfering with Lol system function was predicted to have pleiotropic effects that, when combined, would yield a fatal outcome for the bacterial cell. The most striking effect we observed after Lol system knockdown was the formation of MOMVs filled with periplasm extruding from the cell at sites of plasmolysis. Gram-negative bacteria are known to produce OMVs that play a wide variety of roles, including promoting pathogenesis, surviving stress, and interacting with other bacteria in communities, and, because of their versatility, OMVs have been used as a platform for bioengineering applications. However, the underlying mechanism of OMV production remains to be fully understood. In *E. coli*, loss of the covalent linkage of the OM to PG through Lpp leads to increased OMV production (31). Additionally, proteinaceous waste may be shed via OMVs as is the case when stressors lead to the periplasmic accumulation of misfolded protein (21, 31). The OMVs described in this study are on average four times larger than OMVs previously described; we hence propose the term "mega" OMV or MOMV. While it is possible that OMV and MOMV formation share no common mechanism, some similarities in origin and function may exist (see *SI Appendix*, Fig. S17 for a model of MOMV formation). For example, during Lol system knockdown, failure to transport Lpp to the OM likely leads to reduction in OM-PG linkages and thus MOMV formation. Additionally, the BAM complex relies on lipoprotein transport since four of its integral components are lipoproteins. Failure to assemble β-barrel proteins at the OM leads to their toxic accumulation in the periplasm (32). MOMVs, which are filled with periplasm, could play a role in removing this undesirable protein waste accumulating as a consequence of impaired lipoprotein transport, acting as OMVs do during stress responses (32).

It has been shown that perturbing LPS organization on the cell surface induces phospholipid migration from the inner to the outer leaflet of the OM, generating locally symmetrical bilayer rafts that are more permeable to hydrophobic molecules. *V. cholerae* appear to have naturally occurring symmetric bilayer patches (33) and are thus intrinsically more susceptible to some hydrophobic compounds (such as rifampin and novobiocin), but the genetic basis for the formation of these patches is not known. Lol system depletion could in principle exacerbate the formation of these patches by interrupting LPS transport and the maintenance of OM lipid asymmetry through the action of Mla gene products (34). VacJ is the *V. cholerae* MlaA homolog, which is a lipoprotein, and a *vacJ* mutant has been shown to increase OMV production in these bacteria (35). Therefore, failure of these two systems to properly function could lead to increased migration of phospholipids to the OM and the formation of unstable membrane patches from which MOMVs could extrude. The observed increase in membrane permeability in the Lol system knockdown could in turn lead to death.

The MOMVs described here have biotechnology applications since, like OMVs, they could potentially be used as cell-free vaccine platforms that are loaded with engineered or natural antigens, nanoreactors containing enzymatic reaction cascades, or utilized as delivery platforms for targeted human therapeutics. Thus, cell biological insights gained through the knockdown of essential gene expression are likely to have many applications in drug and therapeutic discovery.

Methods

Strains, Media, and Culture Conditions. *V. cholerae* El Tor C6706 CRISPRi strains were grown in Luria–Bertani (LB) Lennox (0.5% NaCl). The CRISPRi screen strains were grown in 1.2 mL of media in 96-deep well plates (VWR) at 37 °C shaking at 900 rpm overnight. CRISPRi gene knockdown was induced with anhydrotetracycline (aTc) (Sigma Aldrich) at 10 nM or 50 nM for cultures in exponential or stationary phase, respectively. Carbenicillin (Sigma Aldrich) was used at 100 $\mu g \cdot mL^{-1}$ to select for the sgRNA-expressing plasmid.

Strain Construction and sgRNA Selection and Cloning. *S. pyogenes* dCas9 under the control of a tetracycline inducible promoter (P_{tet}) was amplified from pdCas9-bacteria (44249; Addgene) and introduced into the *V. cholerae* nonessential lacZ locus (*vc2338*). The major OM lipoprotein Lpp (*vca059*) gene was deleted in-frame leaving the three first and last codons. Lpp homology regions were Gibson assembled into the pDS132 plasmid using primers oFC589-592. Genetic modifications were performed as previously described (36). SgRNAs were designed using the "find CRISPR sites tool" in the Geneious R11 software using the specificity and activity score settings to find a 20- to 25-nt target sequence and NGG PAM site in the *V. cholerae* N16961 reference genome used also as the off-target database. SgRNAs were cloned as previously described (12) and are listed in *SI Appendix*, Table S1. Briefly, inverse PCR was performed on the pgRNA-bacteria plasmid (44251; Addgene) using primers containing a plasmid-specific region and the sgRNA sequence. The sgRNA plasmid obtained was electroporated into *V. cholerae* and selected using carbenicillin. The PAM_{mut} strain was generated by homologous recombination for mutation of the sg-*lolC* PAM from TGG to TCG. Both cytoplasmic sfGFP and ^{SS}dsbA-sfGFP under the control of an arabinose-inducible promoter (P_{BAD}) were amplified from the pBAD24 vector using primers oFC613 and oFC719 for Gibson assembly into the

sgRNA XhoI site. To fluorescently tag the OM, we used a synthetic oligo encoding the first 22 amino acids of *V. cholerae* Lpp followed by a 6 (3× Ala, 3× Gly) amino acid linker fused to mCherry to yield ^{SS}lpp-mCherry, which was cloned into the EcoRI and HindIII sites of pBAD24. To create sgRNA-^{SS}dsbA-sfGFP-^{SS}lpp-mCherry, ^{SS}dsbA-sfGFP was amplified using primers oFC743 and oFC744 from the sgRNA-^{SS}dsbA-sfGFP and Gibson assembled into the sgRNA-^{SS}lpp-mCherry XhoI site for simultaneous expression of both fluorescent proteins. For detailed sequences, see *SI Appendix*, Table S1.

CRISPRi Knockdown Viability. For exponential phase gene knockdown, overnight cultures were back-diluted 100-fold, grown for 2 h until $OD_{600} \sim 0.5$, and 10-fold serial dilutions were spotted onto LB agar with or without 10 nM aTc. For stationary phase gene knockdown, overnight cultures were grown for 5 h in the presence or absence of 50 nM aTc and then plated onto LB agar without aTc. To obtain the growth curves in *SI Appendix*, Fig. S3, each strain was streaked on agar plates and grown overnight at 37 °C. On 3 separate days, 1 colony of each strain was inoculated into 1.2 mL of media in deep 96-well plates and grown shaking at 900 rpm for 4 h to OD_{600} ~0.5. Cultures were diluted to 2.5×10^6 cells·mL^{-1}, and 20 μL were aliquotted into 4 wells of a 384-well plate (50,000 cells per well) that contained 20 μL of media with or without 20 nM aTc. OD_{600} measurements were taken every 2 min for 20 h, shaking continuously at 37 °C on the BioTek's Synergy Mx Microplate Reader. This was repeated on 3 separate days to obtain a total of 12 growth curves, 3 true biological replicates with 4 technical replicates for each of the strains grown in each condition. The same procedure was applied to the growth curves displayed in Fig. 1*E* but aliquotting 500 cells per well.

RNA-Seq. To obtain stationary and exponential phase transcriptomes, RNA was extracted from overnight cultures or exponentially growing bacteria at $OD_{600} \sim 0.5$ using the PureLink RNA mini kit (Invitrogen) according to the manufacturer's instructions. RNA-seq libraries were prepared using the Ovation Complete Prokaryotic RNA-Seq library kit (NuGEN) following the manufacturer's instructions. Libraries were sequenced at the Biopolymers Facility at Harvard Medical School using an Illumina HiSeq 2500. Then, 4,036,728 and 4,038,703 reads for stationary and exponential phase bacteria, respectively, were mapped to the *V. cholerae* N16961 reference genome, and TPM (Transcripts per Million = [CDS read count × mean read length × 106]/[CDS length × total transcript count]) were calculated using the Geneious 11.1.4 software package.

qRT-PCR. Cells were harvested and resuspended in 1 mL of TRIzol (Invitrogen) and incubated for 5 min at room temperature before adding 200 μL of chloroform. Samples were centrifuged at 13,000 relative centrifugal field (rcf) for 10 min. The aqueous phase was mixed with 200 μL of 100% ethanol and transferred to Purelink RNA Mini columns (Invitrogen) for purification following the manufacturer's instructions. RNA was treated with TURBO DNase (Invitrogen) according to the manufacturer's instructions. The KAPA SYBER FAST One-Step qRT-PCR Kit (Kapa Biosystems) was used to measure mRNA abundance on the Eppendorf Mastercycler RealPlex2 system. Relative gene expression changes were calculated using the Livak method (37).

Electron Microscopy. Bacteria were grown for 30 min in the presence of 10 nM aTc and harvested by centrifugation. The pellet was resuspended in 1× PBS and fixed in 2.5% Glutaraldehyde, 1.25% Paraformaldehyde, and 0.03% picric acid in 0.1 M sodium cacodylate buffer (pH 7.4), and ultrathin sections were prepared and imaged following instructions provided by the Electron Microscopy Facility at Harvard Medical School. Sections were examined using a JEOL 1200EX Transmission electron microscope or a TecnaiG^2 Spirit BioTWIN.

Microfluidics and Time-Lapse Microscopy. Exponential phase bacteria were transferred into the cell wells of the CellASIC ONIX Microfluidic Plates (Millipore), loaded into the microfluidics chambers following the manufacturer's instructions, and perfused with medium at 2 psi flow rate. Plates were kept at 37 °C for the duration of the experiment inside a Nikon Ti-S/U/E Environmental Chamber. Alternatively, bacteria were transferred onto 1.5% agarose pads made in M9, 100 μM $CaCl_2$, 2 mM $MgSO_4$, 0.4% glycerol, plus or minus the corresponding test compounds, which were added directly into the melted agarose at 55 °C immediately before preparing the pads. Images were recorded using a Nikon Ti-E inverted motorized microscope with Perfect Focus System and a Plan Apo 100× Oil Ph3 DM (NA 1.45) objective lens. Lumencor SPECTRA X3 light engine, ET-EGFP (Ex 470/40 nm, Ex 525/50 nm), and ET-DSRed (Ex 545/30 nm, Ex 620/60 nm), ZYLA 4.2-CL 10 sCMOS Camera and NIS Elements 4.0 were used to record images.

ACKNOWLEDGMENTS. We thank T. Dougherty, D. Kahne, T. Bernhardt, and D. Rudner for helpful discussion. This work was supported by NIH/National Institute of Allergy and Infectious Diseases Grant R01AI018045 (to J.J.M.).

1. A. H. Delcour, Outer membrane permeability and antibiotic resistance. *Biochim. Biophys. Acta* **1794**, 808–816 (2009).
2. M. Grabowicz, Lipoprotein transport: Greasing the machines of outer membrane biogenesis: Re-examining lipoprotein transport mechanisms among diverse gram-negative bacteria while exploring new discoveries and questions. *BioEssays* **40**, e1700187 (2018).
3. K. Masuda, S. Matsuyama, H. Tokuda, Elucidation of the function of lipoprotein-sorting signals that determine membrane localization. *Proc. Natl. Acad. Sci. U.S.A.* **99**, 7390–7395 (2002).
4. K. Yamaguchi, F. Yu, M. Inouye, A single amino acid determinant of the membrane localization of lipoproteins in E. coli. *Cell* **53**, 423–432 (1988).
5. G.-W. Li, D. Burkhardt, C. Gross, J. S. Weissman, Quantifying absolute protein synthesis rates reveals principles underlying allocation of cellular resources. *Cell* **157**, 624–635 (2014).
6. M. Grabowicz, T. J. Silhavy, Redefining the essential trafficking pathway for outer membrane lipoproteins. *Proc. Natl. Acad. Sci. U.S.A.* **114**, 4769–4774 (2017).
7. T. Yakushi, T. Tajima, S. Matsuyama, H. Tokuda, Lethality of the covalent linkage between mislocalized major outer membrane lipoprotein and the peptidoglycan of Escherichia coli. *J. Bacteriol.* **179**, 2857–2862 (1997).
8. D. E. Cameron, J. M. Urbach, J. J. Mekalanos, A defined transposon mutant library and its use in identifying motility genes in Vibrio cholerae. *Proc. Natl. Acad. Sci. U.S.A.* **105**, 8736–8741 (2008).
9. M. C. Chao *et al*., High-resolution definition of the Vibrio cholerae essential gene set with hidden Markov model-based analyses of transposon-insertion sequencing data. *Nucleic Acids Res.* **41**, 9033–9048 (2013).
10. J. M. Peters *et al*., A comprehensive, CRISPR-based functional analysis of essential genes in bacteria. *Cell* **165**, 1493–1506 (2016).
11. X. Liu *et al*., High-throughput CRISPRi phenotyping identifies new essential genes in *Streptococcus pneumoniae*. *Mol. Syst. Biol.* **13**, 931 (2017).
12. L. S. Qi *et al*., Repurposing CRISPR as an RNA-guided platform for sequence-specific control of gene expression. *Cell* **152**, 1173–1183 (2013).
13. J. Zheng, O. S. Shin, E. D. Cameron, J. J. Mekalanos, Quorum sensing and a global regulator TsrA control expression of type VI secretion and virulence in Vibrio cholerae. *Proc. Natl. Acad. Sci. U.S.A.* **107**, 21128–21133 (2010).
14. H. Zhao *et al*., Depletion of undecaprenyl pyrophosphate phosphatases disrupts cell envelope biogenesis in Bacillus subtilis. *J. Bacteriol.* **198**, 2925–2935 (2016).
15. J. M. Peters *et al*., Bacterial CRISPR: Accomplishments and prospects. *Curr. Opin. Microbiol.* **27**, 121–126 (2015).
16. H. D. Kamp, B. Patimalla-Dipali, D. W. Lazinski, F. Wallace-Gadsden, A. Camilli, Gene fitness landscapes of Vibrio cholerae at important stages of its life cycle. *PLoS Pathog.* **9**, e1003800 (2013).
17. B. R. Levin, D. E. Rozen, Non-inherited antibiotic resistance. *Nat. Rev. Microbiol.* **4**, 556–562 (2006).
18. L. Cui *et al*., A CRISPRi screen in E. coli reveals sequence-specific toxicity of dCas9. *Nat. Commun.* **9**, 1912 (2018).
19. T. Dörr, F. Cava, H. Lam, B. M. Davis, M. K. Waldor, Substrate specificity of an elongation-specific peptidoglycan endopeptidase and its implications for cell wall architecture and growth of Vibrio cholerae. *Mol. Microbiol.* **89**, 949–962 (2013).
20. T. Dinh, T. G. Bernhardt, Using superfolder green fluorescent protein for periplasmic protein localization studies. *J. Bacteriol.* **193**, 4984–4987 (2011).
21. M. Nakajima *et al*., Globomycin, a new peptide antibiotic with spheroplast-forming activity. III. Structural determination of globomycin. *J. Antibiot. (Tokyo)* **31**, 426–432 (1978).
22. E. Moison *et al*., A fluorescent probe distinguishes between inhibition of early and late steps of lipopolysaccharide biogenesis in whole cells. *ACS Chem. Biol.* **12**, 928–932 (2017).
23. C. Schwechheimer, M. J. Kuehn, Outer-membrane vesicles from gram-negative bacteria: Biogenesis and functions. *Nat. Rev. Microbiol.* **13**, 605–619 (2015).
24. E. Altindis, Y. Fu, J. J. Mekalanos, Proteomic analysis of Vibrio cholerae outer membrane vesicles. *Proc. Natl. Acad. Sci. U.S.A.* **111**, E1548–E1556 (2014).
25. O. Ciofu, T. J. Beveridge, J. Kadurugamuwa, J. Walther-Rasmussen, N. Høiby, Chromosomal beta-lactamase is packaged into membrane vesicles and secreted from Pseudomonas aeruginosa. *J. Antimicrob. Chemother.* **45**, 9–13 (2000).
26. Y. Taniguchi *et al*., Quantifying E. coli proteome and transcriptome with single-molecule sensitivity in single cells. *Science* **329**, 533–538 (2010).
27. J.-R. Wei *et al*., Depletion of antibiotic targets has widely varying effects on growth. *Proc. Natl. Acad. Sci. U.S.A.* **108**, 4176–4181 (2011).
28. J. M. Rock *et al*., Programmable transcriptional repression in mycobacteria using an orthogonal CRISPR interference platform. *Nat. Microbiol.* **2**, 16274 (2017).
29. A. Vigouroux, E. Oldewurtel, L. Cui, D. Bikard, S. van Teeffelen, Tuning dCas9's ability to block transcription enables robust, noiseless knockdown of bacterial genes. *Mol. Syst. Biol.* **14**, e7899 (2018).
30. M. Madan Babu, K. Sankaran, DOLOP–Database of bacterial lipoproteins. *Bioinformatics* **18**, 641–643 (2002).
31. C. Schwechheimer, C. J. Sullivan, M. J. Kuehn, Envelope control of outer membrane vesicle production in Gram-negative bacteria. *Biochemistry* **52**, 3031–3040 (2013).
32. A. J. McBroom, M. J. Kuehn, Release of outer membrane vesicles by Gram-negative bacteria is a novel envelope stress response. *Mol. Microbiol.* **63**, 545–558 (2007).

33. S. Paul, K. Chaudhuri, A. N. Chatterjee, J. Das, Presence of exposed phospholipids in the outer membrane of Vibrio cholerae. *J. Gen. Microbiol.* **138**, 755–761 (1992).
34. J. C. Malinverni, T. J. Silhavy, An ABC transport system that maintains lipid asymmetry in the gram-negative outer membrane. *Proc. Natl. Acad. Sci. U.S.A.* **106**, 8009–8014 (2009).
35. S. Roier *et al*., A novel mechanism for the biogenesis of outer membrane vesicles in Gram-negative bacteria. *Nat. Commun.* **7**, 10515 (2016).
36. V. L. Miller, J. J. Mekalanos, A novel suicide vector and its use in construction of insertion mutations: Osmoregulation of outer membrane proteins and virulence determinants in Vibrio cholerae requires toxR. *J. Bacteriol.* **170**, 2575–2583 (1988).
37. K. J. Livak, T. D. Schmittgen, Analysis of relative gene expression data using real-time quantitative PCR and the 2(-Δ Δ C(T)) method. *Methods* **25**, 402–408 (2001).